NANO LETTERS

LETTER

pubs.acs.org/NanoLett

Modulating Resonance Modes and *Q* Value of a CdS Nanowire Cavity by Single Ag Nanoparticles

Qing Zhang,[†] Xin-Yan Shan,[†] Xiao Feng,[†] Chun-Xiao Wang,[†] Qu-Quan Wang,[*,‡] Jin-Feng Jia,[†,*,§] and Qi-Kun Xue[†]

[†]State Key Laboratory of Low-Dimensional Quantum Physics, Department of Physics, Tsinghua University, Beijing 100084, People's Republic of China

[‡]Department of Physics, Wuhan University, Wuhan 430072, People's Republic of China

[§]Department of Physics, Shanghai Jiao Tong University, Shanghai 200240, People's Republic of China

Supporting Information

ABSTRACT: Semiconductor nanowire (NW) cavities with tailorable optical modes have been used to develop nanoscale oscillators and amplifiers in microlasers, sensors, and single photon emitters. The resonance modes of NW could be tuned by different boundary conditions. However, continuously and reversibly adjusting resonance modes and improving *Q*-factor of the cavity remain a great challenge. We report a method to modulate resonance modes continuously and reversibly and improve *Q*-factor based on surface plasmon-exciton interaction. By placing single Ag nanoparticle (NP) nearby a CdS NW, we show that the wavelength and relative intensity of the resonance modes in the NW cavity can systematically be tuned by adjusting the relative position of the Ag NP. We further demonstrate that a 56% enhancement of *Q*-factor and an equivalent π-phase shift of the resonance modes can be achieved when the Ag NP is located near the NW end. This hybrid cavity has potential applications in active plasmonic and photonic nanodevices.

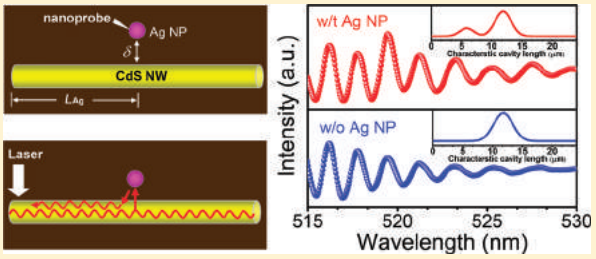

KEYWORDS: Semiconductor nanowire cavity, surface plasmon, CdS nanowire, Ag nanoparticle, *Q*-factor, resonance mode

Optical microcavities, selecting resonance modes and confining light to small volumes, are promising for fabricating integral nanoscale coherent light sources and modulators and show wide range of applications and studies from optical communications, signal processing to imaging.[1,2] With two flat end facets serving as reflecting mirrors and semiconductor material as gain media, one-dimensional semiconductor nanowires (NWs) can be functioned as axial Fabry–Pérot (F-P) cavities.[3,4] Owing to their remarkable properties of the gain media and effective optical waveguides, semiconductor NW F-P cavities have attracted particular interest in microcavities research fields. Up to now, semiconductor NW lasing has been observed in various semiconductors, such as ZnO, GaN, CdS, etc.[1−4]

A high-performance F-P cavity would own resonance modes at precise values and confine light with low loss which can be described by the cavity quality factor *Q*. For semiconductor F-P NW cavity, significant evanescent field exists outside the NW body due to the small diameter of the NW, reducing the reflection of the NW facets and introducing significant losses, thus limiting the *Q*-factor of the cavity to ∼2000. The value is much lower than that of whispering gallery cavity (∼12 000) and hampering the applications of semiconductor cavity.[1,5] Therefore, it is essential for us to develop new methods to tune resonance modes and enhance *Q*-factor of the F-P microcavity. In 2005, Barrelet et al. modulated the resonance modes of CdS NW F-P cavity through embedding the NWs into photonic crystal and racetrack resonator.[6] Recently, by folding CdSe NW to form loop mirrors, Xiao et al. demonstrated a single mode emission microlaser.[7] However, until now continuously and reversibly adjusting resonance modes and improving *Q*-factor of the cavity are still great challenges.

Surface plasmon (SP), the collective oscillation of electrons in conductive bands of metal nanostructures has gained increasing interest due to their capability of manipulating optical processes in nanoscale.[8] Both radiative and nonradiative interband transitions and energy transfer in nanosized optical emitters such as molecules, semiconductor quantum dots and rare-earth nanocrystals have been modified by plasmon-induced strong localized electromagnetic field.[9−15] The detection sensitivity reaches single molecule level in plasmon-enhanced optical spectroscopy.[16−19] In those low-dimensional semiconductor and metal nanosystems, the plasmon−exciton interaction is strong, which can greatly promote the exciton−plasmon−photon conversion. As a result, conversion in single

Received: July 5, 2011
Revised: August 16, 2011
Published: September 06, 2011

ACS Publications © 2011 American Chemical Society

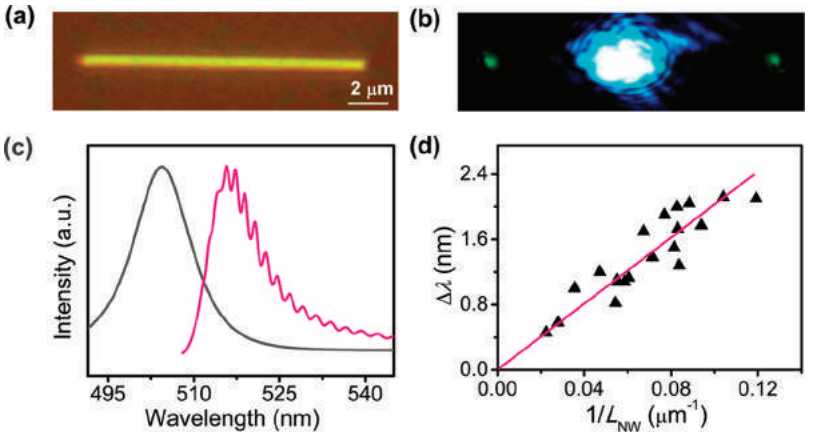

Figure 1. (a) Optical image of a CdS NW. (b) Corresponding PL image when a focused 488 nm laser excites at the middle part of the NW. (c) Normalized PL spectra detected at the excitation position (black line) and the left end of the NW (magenta line). (d) Mode spacing $\Delta\lambda$ at 518 nm versus NW-length for 21 independent straight NWs. Black triangles are experimental points and the red line is the linear fit to the data.

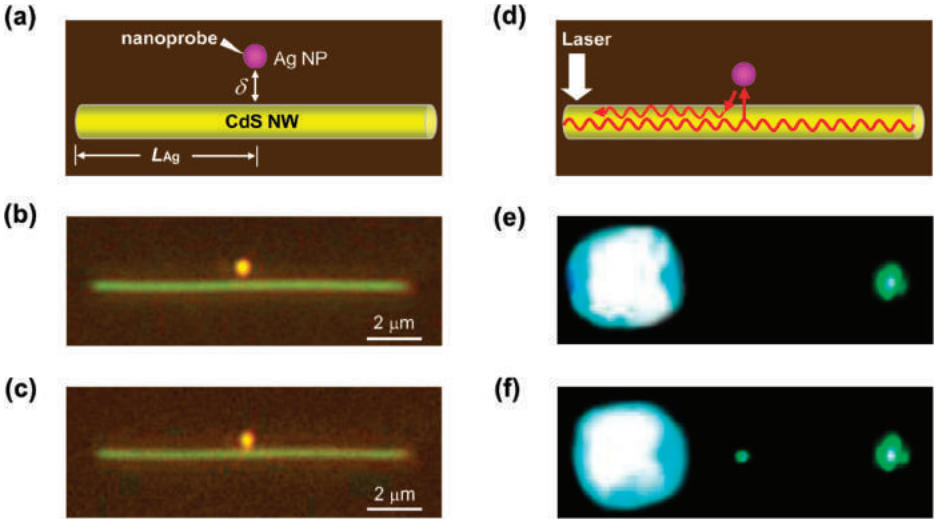

Figure 2. (a) The CdS NW−Ag NP hybrid microcavity fabricated with a nanoprobe. (b,c) Optical images of the CdS NW and the Ag NP. The length and diameter of the CdS NW is 12 μm and 170 nm, respectively. The diameter of the Ag NP is 100 nm. The separations between the Ag NP and the side-surface of CdS NW are 780 nm (b) and 300 nm (c), respectively. (d) Schematic illustration of modulations of PL Fabry−Pérot oscillation in the CdS NW by an Ag NP located nearby the side-surface of the NW. Propagating PL can be reflected backward by the Ag NP. (e,f) Corresponding PL images of the CdS NW with Ag NP depicted in (b,c) when a focused 488 nm laser was excited at the left end of the NW.

quanta level and plasmonic lasing can be achieved based on hybrid metal−semiconductor nanostructures.[16,20−25] Although it was extensively studied that the absorption and emission properties of semiconductor nanostructures could be modified by plasmonic nanostructures, the adjustment of resonance modes and improvement of *Q*-factor of semiconductor nanowire cavity by metal nanostructure have not been reported so far.

In this paper, we report the first experiment of modulating the resonance mode and *Q*-factor of a nanosized optical oscillator by exploiting plasmon-exciton interaction and energy transfer between metal nanoparticle (NP) and semiconductor NW. By placing single Ag NP nearby a CdS NW, we show that the wavelength and relative intensity of the resonance modes in the NW cavity can systematically be tuned by adjusting the relative position of the Ag NP. We further demonstrate a 56% enhancement of Q-factor and an equivalent π-phase shift of the resonance modes can be achieved when the Ag NP is located near the NW end.

The CdS NWs were prepared by vapor transport technique.[26] For optical measurement, the samples were dispersed into ethanol solution and then deposited onto a quartz glass substrate and dried naturally. The Ag NPs were synthesized with polyol method,[27] suspended in alcohol solution and then dropped onto another quartz substrate. The CdS−Ag structures were fabricated by a micromanipulator equipped with a fiber probe (see Figure S1 in Supporting Information), in which single Ag NP on quartz glass substrate was attached by the fiber apex via electromagnetic force, moved and finally released near a CdS NW on another quartz glass substrate. A confocal microscope with a 100× objective (Olympus MPLFLN 100×/0.9) was used to focus a continuous wave laser beam (wavelength at 488 nm, Ar^+ laser produced by Spectra Physics Corporation)

dx.doi.org/10.1021/nl2022674 |*Nano Lett.* 2011, 11, 4270–4274

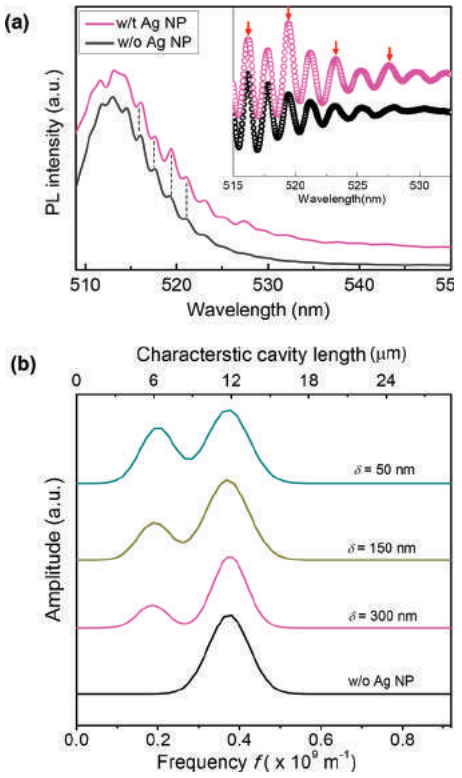

Figure 3. Modulation of Fabry–Pérot oscillations in CdS NW. (a) Normalized PL spectra with Ag NP (magenta line) and without Ag NP (dark line). The dashed lines indicate the wavelengths of the corresponding resonance modes in two situations. The inset shows background-subtracted PL spectra in two situations. Red arrows indicate the enhanced modes in the NW Fabry–Pérot cavity with Ag NP. (b) Fourier transformation of the PL spectra plotted versus reciprocal wavelength when δ = 50 nm, 150 nm, 300 nm, and ∞ (without Ag NP).

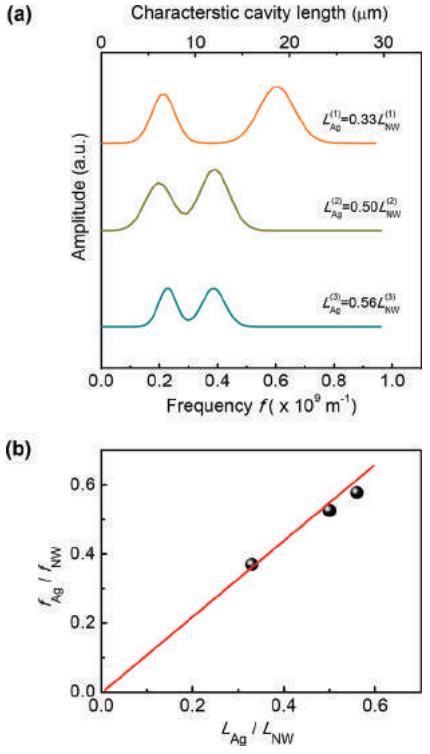

Figure 4. (a) Fourier transformations of PL spectra for three CdS NW–Ag NP structures. The lengths of three CdS NWs are 18.5, 12.0, and 12.0 μm. respectively. L_{Ag} are 0.33 $L_{NW}^{(1)}$, 0.50 $L_{NW}^{(2)}$ and 0.56 $L_{NW}^{(3)}$, respectively. (b) f_{Ag}/f_{NW} as a function of L_{Ag}/L_{NW}. Dark spheres are experiment data, and red line is a linear fit to the data.

on individual NWs. The corresponding focused laser spot is about 1 μm in diameter and the excitation power density is approximately 30 kW/cm^2. The microphotoluminescence (μ-PL) was collected by the same objective and analyzed with a monochromator (SP2750i) and a liquid nitrogen cooled CCD (Princeton instrument, Spec10). For PL spectra measurements, a long pass filter with a 488 nm cutoff wavelength was used to block out the laser. All the measurements were carried out at room temperature.

We first investigated PL waveguide and oscillation in a bare CdS NW. Figure 1a shows an optical image of a CdS NW with a length L_{NW} = 17.0 μm. Figure 1b is the PL image when a 488 nm laser is focused at the middle part of the NW. Two bright green spots can be observed at the two ends of the NW, indicating that the CdS NW has an effective waveguiding property.[3] The μ-PL spectra response at excitation position and the left end of the NW (left green spot) were plotted together in Figure 1c. The PL detected at excitation position has a peak around 505 nm, which is attributed to the band edge emissions of the CdS NW.[3] The PL emitted from the NW end exhibits a main emission peaked around 511 nm, 6 nm red-shifting compared with the PL emission at the excitation position due to the reabsorption of the CdS NW during waveguiding process.[3,28−30] Obvious intensity oscillations are observed in the PL spectrum of NW end, which represent different resonance modes of the NW cavity. The mode spacing (the difference of the two adjacent resonance wavelengths) $\Delta\lambda_R$ varies from 1.55 to 3.42 nm with resonance wavelength increasing from 515 to 558 nm due to dispersion. For a F-P type cavity, $\Delta\lambda_R$ is given by $\lambda_R^2/(2L_{NW}(n_e - \lambda_R(dn_e/d\lambda_R)))$, where λ_R is the resonance wavelength, L is the length of the NW, n_e is the effective refractive index, and $dn_e/d\lambda_R$ is the dispersion relation.[3] For a given λ_R, the mode spacing should be in proportion to the inverse length ($\Delta\lambda_R \propto 1/L_{NW}$). The measured relations $\Delta\lambda_R \sim 1/L_{NW}$ at resonance mode λ_R = 518 nm are presented in Figure 1d, which satisfy the linear relations $\Delta\lambda_R \propto 1/L_{NW}$.

To investigate the modulation of F-P oscillation by SP of metal nanostructure, we move an Ag NP toward a CdS NW, as illustrated in Figure 2a. The position of the Ag NP is labeled by L_{Ag} and δ, where L_{Ag} is the axial distance between the Ag NP and the left end of the CdS NW and δ is the separation between two. Figure 2b,c shows the optical images of a CdS NW and an Ag NP with different δ. The length of the NW L_{NW} = 12.0 μm and $L_{Ag} \approx L_{NW}/2$ = 6.0 μm. The diameters of the NP and the NW are 100 and 170 nm, respectively. The separation δ in Figure 2b is approximately 300 nm measured by using atomic force microscopy (AFM) (see Figure S2 in Supporting Information). Interestingly, when an Ag NP is close to the NW, the photoluminescence (PL) propagating in the NW will be partially reflected by the NP due to plasmon–exciton interaction, as schematically shown in Figure 2d. In this case, the Ag NP acts as a reflecting mirror and creates a new cavity with a length of L_{Ag} in the NW. The resulting resonance modes in the NW are determined by two cavities, and the intensities and wavelengths of the resonance modes can be strongly modulated by the location

dx.doi.org/10.1021/nl2022674 |Nano Lett. 2011, 11, 4270–4274

of the Ag NP (L_{Ag} and δ). Figure 2e,f shows the PL images when the structures depicted in Figure 2b,c are illuminated with a focused 488 nm laser, respectively. When the gap is very large (δ > 700 nm), only one green spot is observed at the right end of the NW, which indicates that the NW is a good waveguide with few surface defects and the interaction between NW and NP is neglected in this case. However, a new green spot is observed at the gap position of Ag−CdS when δ < 300 nm, indicating an exciton−plasmon−photon conversion process reported previously.[14,18−23] It has been investigated that SP-exciton energy transfer can occur based on coulomb interaction when the distance of adjacent metal and semiconductor structure is short enough.

In Figure 3a, we show normalized PL spectra of the CdS NW with (magenta line) and without (dark line) Ag NP, where obvious intensity oscillations can be observed. Each peak in the oscillation characterizes different resonance mode of the NW cavity. The mode spacing (the difference of the two adjacent resonance wavelengths $\Delta\lambda_R$) is 1.63 nm at the resonant wavelength λ_R = 518 nm, fitting well with $\Delta\lambda_R \sim \lambda_R$ curves for CdS NW F-P cavities in Figure 1d. Although the presence of the Ag NP does not change the resonance wavelength (λ_R), it significantly tunes the relative intensity, which is more clearly revealed in the spectra after background subtraction (the insert of Figure 3a). Another interesting observation is that the oscillations exhibit a period of $2\Delta\lambda_R$; every other mode is strongly enhanced, as indicated by the red arrows in the insert of Figure 3a. Because the characteristic length of the NP induced cavity is nearly one-half of that of the bare NW, the observation can preliminarily be understood by the relation $\Delta\lambda_R \propto 1/L$ for a given λ_R in F-P cavity.

The plasmon-modulated resonance modes are further analyzed by Fourier transformation (FT) of PL spectra. The FT frequency f extracted from the PL spectra is equal to the inverse of the mode space (i.e., $f = 1/\Delta\lambda_R$). As shown in Figure 3b, one can see a peak at the FT frequency $f_{NW} = 0.398 \times 10^9\ m^{-1}$ for the bare NW, the corresponding characteristic cavity length L_c is 12.0 μm (= L_{NW}). The peak at $0.20 \times 10^9\ m^{-1}$ (f_{Ag}) is induced by the Ag NP, and the corresponding L_c is 6.0 μm (= L_{Ag}), which strongly supports that the f_{Ag} peak is caused by the Ag NP. Figure 3b also shows that the intensity of the plasmon-induced f_{Ag} peak increases as the gap separation decreases from 300 to 50 nm due to stronger plasmon−exciton interaction at narrower gap in this range (the gap dependent PL spectra are shown in Figure S3 in Supporting Information). It has been extensively reported that the near-field excition−plasmon−photon interaction and energy transfer rate between SP and exciton were enhanced with the decreasing of the gap between metal and semiconductor nanostructures.[31−33]

The resonance modes of the NW F-P cavity can be systematically tuned by manipulating the axial location of the Ag NP L_{Ag}. Three different structures are investigated and the results are shown in Figure 4. From the FT analysis of the PL spectra of three situations, the normalized frequency f_{Ag}/f_{NW} is basically scaled to the normalized axial position L_{Ag}/L_{NW}. Take NW_2 and NW_3 with the same f_{NW} ($0.39 \times 10^9\ m^{-1}$ for an instance, f_{Ag} is $0.22 \times 10^9\ m^{-1}$ ($f_{Ag}/f_{NW} = 0.56$) and $0.20 \times 10^9\ m^{-1}$ ($f_{Ag}/f_{NW} = 0.51$) when L_{Ag}/L_{NW} is manipulated to be 0.56 and 0.50, respectively. The linear relationship between f_{Ag}/f_{NW} and L_{Ag}/L_{NW} is clearly demonstrated in Figure 4b. These observations consistently confirm that the NP plasmon-induced resonance modes are indeed attributed to a cavity with a length of L_{Ag}, which can be manipulated as shown above.

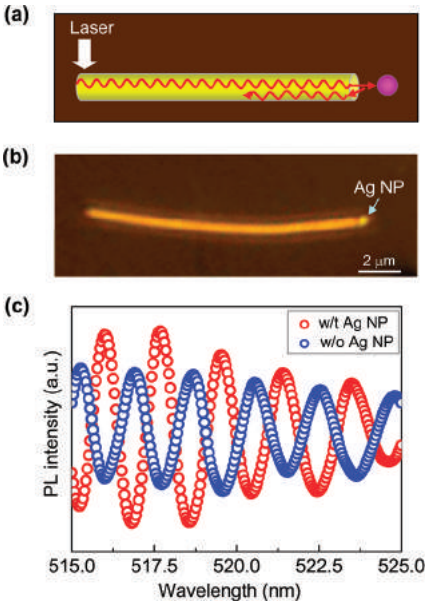

Figure 5. (a) Schematic illustration of modulation of Fabry-Pérot oscillations in the CdS NW by an Ag NP located near the NW end. (b) Optical image of the CdS NW with an Ag NP. (c) Normalized PL spectra (background subtracted) at the right end of the NW in the presence or absence of Ag NP when a focused 488 nm laser is illuminated at the middle part of the NW.

Finally, we show that the Q-factor and the phase of the CdS NW cavity can be modulated by the Ag NP too. When an Ag NP is placed near the right end of the CdS NW (see Figure 5a), the NP acts as a nanomirror and enhances the reflection of the right end-facet of the NW so that the Q-factor of the NW can be increased. As shown in Figure 5b, the separation between the Ag NP and the CdS NW is approximately 150 nm. The PL spectra at the right end of the NW was recorded when a laser illuminated at the middle part of the NW. In the presence of the NP, the full width at half-maximum (fwhm) of the resonance mode at 517.6 nm decreases to approximately 0.53 nm, corresponding to a Q-factor ~1000 ($Q = \lambda/\lambda_{fwhm}$ for a typical F-P cavity[1]), which is ~56% larger than that of the bare CdS NWs ($Q \approx 640$ at 515 nm in the absence of Ag NP). It is because that the Ag NP reflects back PL leaked out at the NW end and reduces cavity energy loss. The enhancement of Q-factor is attributed to the strong near-field exciton−plasmon interaction. Note that even though the Q-factor is enhanced, it is still much lower than that of the other types of cavity.[1] The size and distance of the structure would be critical to obtain a higher enhancement on Q-factor. Previous studies show that shorter distance will lead to stronger plasmon−exciton interaction, however if the distance is smaller than 5 nm the PL would be quenched which may hamper the Q-factor.[31,34,35] Therefore a distance of 5−20 nm would induce a stronger dipole−dipole resonance interaction and give a much higher Q-factor enhancement. One more interesting observation is that the resonance wavelength λ_R shifts about half the period of the mode space (i.e., $\Delta\lambda/2$) as show in Figure 5c. This means that an equivalent π-phase shift is induced by the Ag NP. According to the work of Prikulis et al.,[36] the phase shift may be induced by the retardation of Ag NP. The scattering peak of the Ag NP with a diameter of ~100 nm in our experiments was measured to be about 529 nm (see Figure S5 in Supporting Information), which

dx.doi.org/10.1021/nl2022674 |Nano Lett. 2011, 11, 4270–4274

is at the red side of the resonance modes (518 nm), and the phase shift could be as large as π.

Therefore, Ag NP can simultaneously modulate the effective cavity length, equivalent phase shift, and the Q factor of the cavity modes. Ag NP acts as a reflective and half-reflective nanomirror when it is located at the end of and at the side of the CdS NW cavity, respectively. Our observations provide a new approach to adjusting the resonances modes and improving corresponding Q-factor of semiconductor NW cavities via exciton-plasmon interaction, which may find applications in active plasmonic nanodevices, such as plasmon assisted nanolasers and nanosensors.

■ ASSOCIATED CONTENT

Supporting Information. Additional information and figures.This material is available free of charge via the Internet at http://pubs.acs.org.

■ AUTHOR INFORMATION

Corresponding Author

*E-mail: (Q.-Q.W.) qqwang@whu.edu.cn; (J.-F.J.) jfjia@sjtu.edu.cn.

■ ACKNOWLEDGMENT

We thank Li Zhou and Min Li for the sample preparation, Zhong-Jian Yang and Zong-Suo Zhang for the assistance in FDTD simulations, Jing-Yun Gao for the preparation of glass fiber tips, and Xin-Feng Liu for helpful discussion. This work was supported by NSFC and National Program on Key Science Research of China (2007CB935300).

■ REFERENCES

(1) Vahala, K. J. *Nature* **2003**, *424*, 839–846.
(2) Yokoyama, H. *Science* **1992**, *256*, 66–70.
(3) Duan, X. F.; Huang, Y.; Agarwal, R.; Lieber, C. M. *Nature* **2003**, *421*, 241–245.
(4) Huang, M. H.; Mao, S.; Feick, H.; Yan, H. Q.; Wu, Y. Y.; Kind, H.; Weber, E.; Russo, R.; Yang, P. D. *Science* **2001**, *292*, 1897–1899.
(5) Zhang, Y. A.; Loncar, M. *Opt. Express* **2008**, *16*, 17400–17409.
(6) Barrelet, C. J.; Bao, J. M.; Loncar, M.; Park, H. G.; Capasso, F.; Lieber, C. M. *Nano Lett.* **2006**, *6*, 11–15.
(7) Xiao, Y.; Meng, C.; Wang, P.; Ye, Y.; Yu, H. K.; Wang, S. S.; Gu, F. X.; Dai, L.; Tong, L. M. *Nano Lett.* **2011**, *11*, 1122–1126.
(8) Gramotnev, D. K.; Bozhevolnyi, S. I. *Nat. Photonics* **2010**, *4*, 83–91.
(9) Galloway, C. M.; Etchegoin, P. G.; Le Ru, E. C. *Phys. Rev. Lett.* **2009**, *103*, 063003.
(10) Govorov, A. O.; Lee, J.; Kotov, N. A. *Phys. Rev. B* **2007**, *76*, 125308.
(11) Lakowicz, J. R. *Anal. Biochem.* **2001**, *298*, 1–24.
(12) Muskens, O. L.; Treffers, J.; Forcales, M.; Borgstrom, M. T.; Bakkers, E.; Rivas, J. G. *Opt. Lett.* **2007**, *32*, 2097–2099.
(13) Pacifici, D.; Lezec, H. J.; Atwater, H. A. *Nat. Photonics* **2007**, *1*, 402–406.
(14) Schietinger, S.; Aichele, T.; Wang, H. Q.; Nann, T.; Benson, O. *Nano Lett.* **2010**, *10*, 134–138.
(15) Wei, H.; Ratchford, D.; Li, X. Q.; Xu, H. X.; Shih, C. K. *Nano Lett.* **2009**, *9*, 4168–4171.
(16) Kinkhabwala, A.; Yu, Z. F.; Fan, S. H.; Avlasevich, Y.; Mullen, K.; Moerner, W. E. *Nat. Photonics* **2009**, *3*, 654–657.
(17) Kneipp, J.; Kneipp, H.; Kneipp, K. *Chem. Soc. Rev.* **2008**, *37*, 1052–1060.
(18) Nie, S. M.; Emory, S. R. *Science* **1997**, *275*, 1102–1106.
(19) Qian, X. M.; Nie, S. M. *Chem. Soc. Rev.* **2008**, *37*, 912–920.
(20) Akimov, A. V.; Mukherjee, A.; Yu, C. L.; Chang, D. E.; Zibrov, A. S.; Hemmer, P. R.; Park, H.; Lukin, M. D. *Nature* **2007**, *450*, 402–406.
(21) Bellessa, J.; Bonnand, C.; Plenet, J. C.; Mugnier, J. *Phys. Rev. Lett.* **2004**, *93*, 036404.
(22) Fedutik, Y.; Temnov, V.; Woggon, U.; Ustinovich, E.; Artemyev, M. *J. Am. Chem. Soc.* **2007**, *129*, 14939–14945.
(23) Govorov, A. O.; Bryant, G. W.; Zhang, W.; Skeini, T.; Lee, J.; Kotov, N. A.; Slocik, J. M.; Naik, R. R. *Nano Lett.* **2006**, *6*, 984–994.
(24) Lee, J.; Hernandez, P.; Lee, J.; Govorov, A. O.; Kotov, N. A. *Nat. Mater.* **2007**, *6*, 291–295.
(25) Oulton, R. F.; Sorger, V. J.; Zentgraf, T.; Ma, R. M.; Gladden, C.; Dai, L.; Bartal, G.; Zhang, X. *Nature* **2009**, *461*, 629–632.
(26) Hoang, T. B.; Titova, L. V.; Jackson, H. E.; Smith, L. M.; Yarrison-Rice, J. M.; Lensch, J. L.; Lauhon, L. J. *Appl. Phys. Lett.* **2006**, *89*, 123123.
(27) Gong, H. M.; Zhou, L.; Su, X. R.; Xioo, S.; Liu, S. D.; Wang, Q. Q. *Adv. Funct. Mater.* **2009**, *19*, 298–303.
(28) Lu, W.; Lieber, C. M. *J. Phys. D: Appl. Phys.* **2006**, *39*, R387–R406.
(29) Yang, P. D. *MRS Bull.* **2005**, *30*, 85–91.
(30) Ninomiya, S.; Adachi, S. *J. Appl. Phys.* **1995**, *78*, 1183–1190.
(31) Anger, P.; Bharadwaj, P.; Novotny, L. *Phys. Rev. Lett.* **2006**, *96*, 113002.
(32) Liu, G. L.; Long, Y. T.; Choi, Y.; Kang, T.; Lee, L. P. *Nat. Methods* **2007**, *4*, 1015–1017.
(33) Fofang, N. T.; Grady, N. K.; Fan, Z. Y.; Govorov, A. O.; Halas, N. J. *Nano Lett.* **2011**, *11*, 1556–1560.
(34) Dulkeith, E.; Ringler, M.; Klar, T. A.; Feldmann, J.; Javier, A. M.; Parak, W. J. *Nano Lett.* **2005**, *5*, 585–589.
(35) Gueroui, Z.; Libchaber, A. *Phys. Rev. Lett.* **2004**, *93*, 166108.
(36) Prikulis, J.; Xu, H.; Gunnarsson, L.; Käll, M.; Olin, H. *J. Appl. Phys.* **2002**, *92*, 6211–6214.